

## Article

# Computerized Data Interpretation for Concrete Assessment with Air-Coupled Impact-Echo: An Online Learning Approach

Jiaxing YE <sup>1,†</sup> , Takumi Kobayashi <sup>1,‡</sup> and Masaya Iwata <sup>1,‡</sup> and Hiroshi Tsuda <sup>1,†</sup> and Masahiro Murakawa <sup>1,‡\*</sup>

<sup>1,†</sup> National Metrology Institute of Japan (NMIJ), The National Institute of Advanced Industrial Science and Technology (AIST), {jiaxing.you, hiroshi – tsuda}@aist.go.jp

<sup>1,‡‡</sup> Artificial Intelligence Research Center (AIRC), The National Institute of Advanced Industrial Science and Technology (AIST), {takumi.kobayashi, m.iwata, m.murakawa}@aist.go.jp

\* Correspondence: jiaxing.you@aist.go.jp; Tel.: +81-29-861-2850

**Abstract:** Developing efficient Artificial Intelligence (AI)-enabled system to substitute human role in non-destructive testing is an emerging topic of considerable interest. In this study, we propose a novel impact-echo analysis system using online machine learning, which aims at achieving near-human performance for assessment of concrete structures. Current computerized impact-echo systems commonly employ lab-scale data to validate the models. In practice, however, the echo patterns can be far more complicated due to varying geometric shapes and materials of structures. To deal with a large variety of unseen data, we propose a sequential treatment for echo characterization. More specifically, the proposed system can adaptively update itself to approaching human performance in impact-echo data interpretation. To this end, a two-stage framework has been introduced, including echo feature extraction and the model updating scheme. Various state-of-the-art online learning algorithms have been reviewed and evaluated for the task. To conduct experimental validation, we collected 10940 echo instances from multiple inspection sites with each sample had been annotated by human experts with healthy/defective condition labels. The results demonstrated that the proposed scheme achieved favorable echo pattern classification accuracy with high efficiency and low computation load.

**Keywords:** non-destructive evaluation; hammering inspection; audio signal processing; machine learning; online learning

## 1. Introduction

Aging infrastructure poses the significant challenges to human society. It is indispensable to perform the efficient non-destructive evaluation (NDE) to ensure the safety of those critical structures. In this study, we focus on hammering impact-echo test, which is one of the most conventional NDE methods for assessment of concrete structures due to the low-cost and high-efficiency [1,2]. In the setting of hammering inspection, field engineer generates surface impact using a handy hammer and then determine structural condition by listening to the echoes. It is evident that such judgment is highly subjective and relies on individual experience; and thus, leaves the evaluation results open to human error. Extensive research efforts had been made to develop efficient computerized echo investigation systems to alleviate human efforts in hammering echo analysis, as well as to eliminate the human-made errors, [4,11,14].

Typical computerized impact-echo analysis system consists of two parts, the impact-echo hardware and data analysis computing system [15,16]. Impact on the surface produces P- and S-waves that traveled into the target structure. Then the echoes are captured by a transducer nearby, i.e., an air-coupled microphone. Through data acquisition (DAQ) process, the data is analyzed by a program,

33 and condition assessment result is presented. Figure 1 shows the schematic flow. This paper mainly  
34 addresses the issue of devising efficient machine learning algorithm for impact-echo.

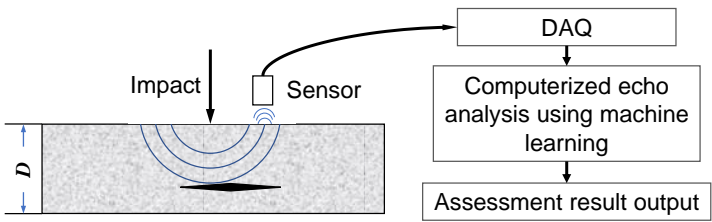


**Figure 1.** The general processing flow of computerized hammering echo investigation

35 Current learning schemes applied for the impact-echo test are restricted to the standard batch  
36 setting, which assumes both training and input testing echo samples reside in the same feature space  
37 with the static statistical characteristic; hence, model training can be performed over the pre-collected  
38 laboratory-scale echo database [11,15,16]. In practices, however, such assumption does not hold. The  
39 patterns of echo signal can alter significantly with the specifications of concrete structures under  
40 evaluation, such as material, shape and years of service [1]. From the viewpoint of machine learning,  
41 these factors would make the posterior distribution of the test echoes drift from that of the pre-collected  
42 training samples; thus, degrading the echo analysis performance.

43 In this study, we adopt an alternative hypothesis which admits the pre-collected training echo  
44 dataset only covers small range of the *complete* distribution; moreover, we propose a new formulation of  
45 echo pattern classification with the online learning paradigm, where efficient model updating schemes  
46 has been exploited to minimize the cumulative prediction loss suffered along with the continuous  
47 input of echo data with expert labels. Online learning is a well-established learning scheme which  
48 has both theoretical and practical appeals [17,18] and it is particularly well-suited to the hammering  
49 impact-echo, since the large-scale echo data can be accessed only in a sequential way.

50 It is noteworthy that our ultimate goal is to develop an efficient hammering echo investigation  
51 system with near-human accuracy. In hammering test, humans are capable of discerning the  
52 defect-induced echoes of various concrete structures by auditory perception. In this study, we propose  
53 AI-enabled computing system by adopting a formulation of binary classification, which produces  
54 labels to indicate healthy or defective concrete, respectively. At validation stage, a loss between the  
55 predicted results and expert labels has been employed to compare the performance of proposed  
56 approach to that of humans. The main contributions of proposed approach can be summarized as  
57 follows:

- 58 • The objective of this study is to build efficient impact-echo analysis system for concrete structure  
59 assessment. To this end, a novel online learning framework had been proposed, which can  
60 effectively characterize discriminant information from large-scale echo spectrum data in an  
61 incremental way.
- 62 • Various state-of-the-art online learning algorithms has been reviewed and evaluated for the  
63 application of hammering echo pattern classification. The side-by-side comparison results can  
64 inspire other applications with streaming data input, not limited to echo signal analysis discussed  
65 in this study.
- 66 • Unlike conventional studies which commonly conduct experiment on laboratory-scale data, a  
67 massive hammering echo database has been created during this study, which includes more than  
68 ten thousand echo samples collected from different types of concrete structures. Moreover, each  
69 echo instance has been annotated by professional inspectors with healthy/defective label. The  
70 database laid solid fundamental for learning scheme validation.

## 2. Related work

In this section, we present a review to the previous studies conducted on hammering impact-echo methods for concrete condition assessment. The review comes up with two parts: the first is fundamental research towards impact-echo method and the latter is recent advances in developing computerized hammering echo investigation system with machine learning techniques.

### 2.1. Impact-echo Method and Air-coupled Hammering Inspection

The initial literatures describing impact-echo presented from 1970s, subsequently, more studies were carried out in both theoretical and experimental aspects [2,3,6]. Echo signal analysis is commonly performed through Fourier analysis. Although advanced methods have been employed in recent works, such as using Wavelet transform [5] to alleviate poor time-frequency resolution in Fourier spectra and fuse impulse response with 3D laser scanning for delamination detection [10], Fourier analysis still dominates in practice due to the efficient implementation. In figure 2, we present one example clip of hammering echo waveform and its Fourier spectrum, respectively.

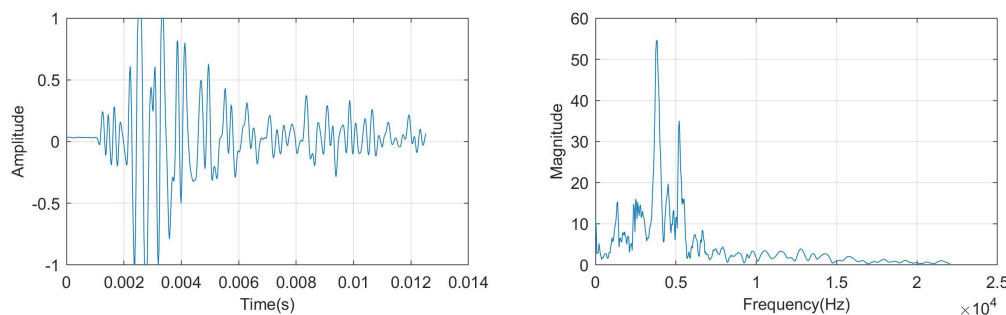


**Figure 2.** Hammering echo waveform (left) and its Fourier spectrum (right)

A well-known formula to determine a void beneath surface of concrete is proposed by [1]:

$$d = \beta \frac{C_p}{2f_{peak}} \quad (1)$$

where  $f_{peak}$  denotes peak frequency of echo signal spectrum,  $C_p$  is the velocity of the longitudinal,  $\beta$  is constant of 0.96 for plate-shape structures wave according to [1] and  $d$  represents depth of inside void. However, some recent studies reveal the availability of formula (1) is constrained by the size and flatness of defect area, e.g. if void is not parallel to surface, the echo resonance behaves differently and thus Equation 1 fails to estimate void depth [9]. In addition, to facilitate engineers' usage of impact-echo technique, imaging methods for impact-echo test attracted much research interests, such as in [7], a depth spectrum is proposed which interprets spectral peak of echo signal to depth of defect. Impact-echo is initially a contact inspection method, which is quite time-consuming to fix transducer, especially when dealing with large structures. To enhance the efficiency, a new suggestion is to apply air-coupled sensor in impact-echo [8]. A designated air-couple sensor is employed to capture acoustic echo from concrete structure. And experimental results show the air-coupled sensor is comparable to contact sensors for delamination detection and grouting quality evaluation tasks. Until now, impact-echo method, due to its high diagnosis accuracy and favorable stability, remains to be active research topic in the non-destructive test field, and efforts will be continuously delivered to the topic.

## 2.2. Data-driven Impact-echo System for Non-destructive Test of Concrete Structure

The last five years have seen remarkable progress in machine learning research, and a spreading trend emerged to develop human-level machine learning systems to relieve people from laborious and exhausting tasks in the structural health monitoring field [4,14]. In order to substituting human role in hammering echo interpretation, great efforts had been carried out to establish data-driven machine learning system to discern anomalous echoes from healthy ones [11,15,16]. We present a review on current status of computerized impact-echo system development as follows.

The early systems commonly tackle echo investigation problem with statistical pattern classification, in which the echo spectra has been used as feature vector and various conventional classifiers have been employed, such as Gaussian mixture models (GMM) [11], Artificial Neural Network (ANN) [12] and Support Vector Machines (SVM) [13], to characterize discriminant information of healthy/defective echoes. In recent years, significant progress has been made in noise robust echo feature representation learning. Advanced echo signal descriptors developed by the bag-of-words model (BoW model) [15] and sparse coding approaches [16] has been proved to be effective for anomalous echo identification under hostile acoustic environment. It is noteworthy that these literatures commonly assume that all training and test echo instances are sampled from same population; the experimental dataset was confined to be the laboratory-scale as well. It is anticipated to be problematic when we directly apply the echo analysis model trained by lab-scale data to practical impact-echo test, because the pre-collected training data is quite limited to render sufficient discriminant information to deal with complex real-world echo patterns.

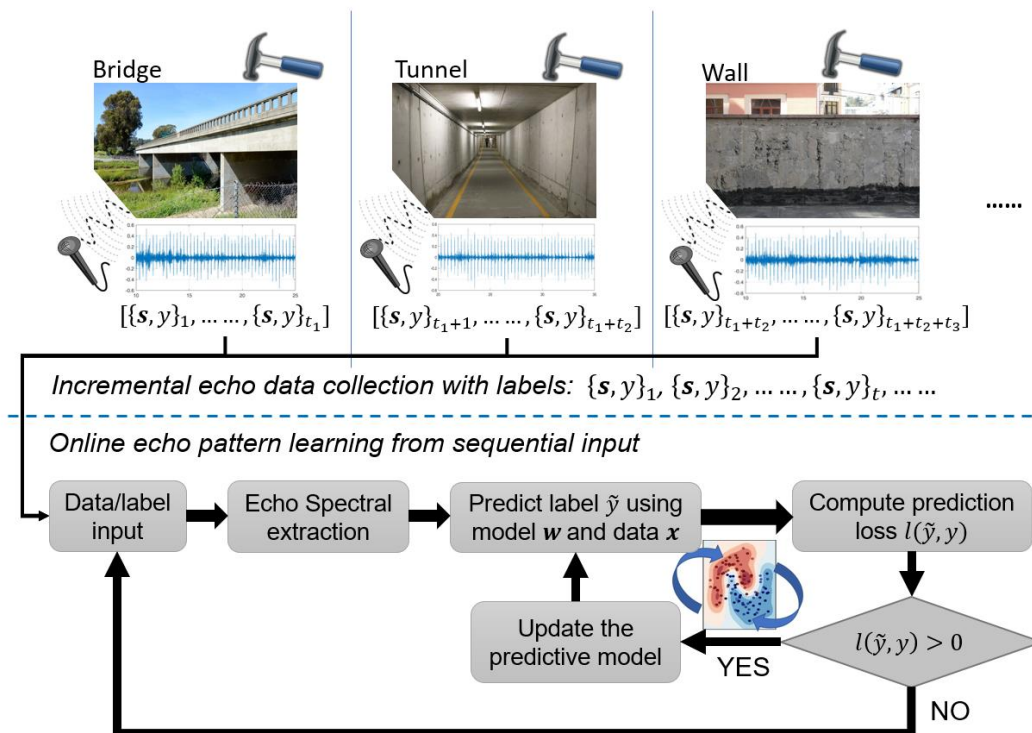


Figure 3. Flow chart of online learning formulation for hammering echo investigation

## 3. The Proposed Online Learning Framework for Hammering Echo Pattern Analysis

We introduce the details of proposed online machine learning-enabled hammering echo analysis system in this section. The processing flow has been shown in figure 3. We assume that the echo instances are received in a streaming way  $\{x, y\}_t, t \in [1, \dots, T]$  and all echoes had been annotated by professional inspector with healthy or anomalous labels. Notably, during the data collection, the

material, shape, and other specifications of target structures can vary from place to place. For instance, in Figure 3 the inspection place shifted from bridge to tunnel, meanwhile the captured echo data/label indexes range varied from  $1 \sim t_1$  to  $t_1 + 1 \sim t_1 + t_2$ , respectively. Our goal is to continuously update the echo analysis model so as to achieve near-human performance for anomalous echo identification. To this end, it is crucial to devise the efficient online learning scheme and various state-of-the-art algorithms have been reviewed and compared. The details are presented as follows.

### 3.1. Echo Feature Extraction

Over decades, spectral analysis has been a dominant approach for hammering echo analysis [3], [6], in which Fourier transform (FT) is employed to generate the spectrum of echo signal. Then, further pattern investigation can be performed. The Fourier analysis can be expressed as:

$$x(f) = \int_{-\inf}^{\inf} s(t)e^{-2\pi ift} dt \quad (2)$$

where  $s(t)$  is echo waveform to be analyzed and  $x(f)$  is the extracted echo spectrum. In the following contents, we will use  $\mathbf{x}_t \in \mathbb{R}^d$  to denote hammering echo spectrum collected at time stamp  $t$ , with  $d$  frequency-bins. Our pattern classification process is based on Fourier spectrum representation of echo signal. In figure 4, we present two examples of echo Fourier spectrum, which were collected from normal and defective concrete structures, respectively. According to the plots, differences in spectral distributions can be clearly observed. In addition, at low frequency region below 500Hz, high noise power can be seen which is irrelevant to hammering specimen. We employed high pass filter to eliminate the ambient noises presented in the band lower than 500Hz. Meanwhile, to reduce echo feature dimension, we also discard the frequency bands higher than 15kHz, since there existed no discriminant information in echo data.

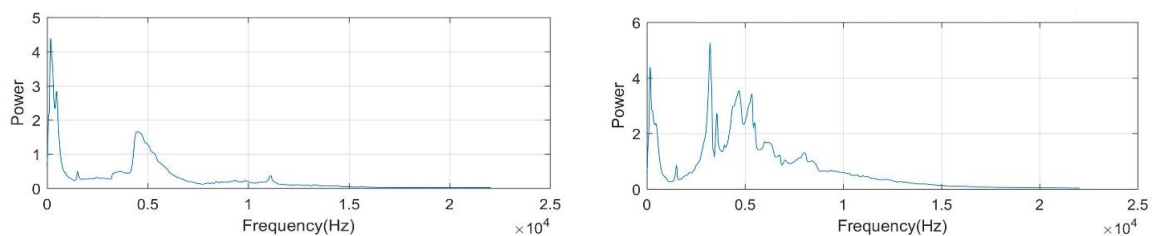


**Figure 4.** Examples of hammering echo spectrum: normal echo (left) and defective case (right)

### 3.2. Online Learning Algorithms in Evaluation

As the core feature of this research, online learning algorithms are employed to deal with the case that hammering echo data (with expert annotations) arrives incrementally with time stamps. Concretely, at time  $t$ , the online learning algorithm analyses the input hammering echo feature vector and expert label, i.e.  $\{\mathbf{x}_t, y_t\}$ , through three steps: the first is to predict its label  $\hat{y}_t \in \{-1, +1\}$ , in which the two digits represent defective and healthy status, respectively. Then, we compare the predicted label  $\hat{y}_t$  with true label  $y_t \in \{-1, +1\}$  by using a well-defined loss function  $l(y_t, \hat{y}_t)$ . Finally, if the computed prediction loss exceeds a threshold, the classification model will be updated in an analytical way. Overall, the cumulative mistake through whole data stream can be minimized. In this section, we first present a general algorithmic framework of online machine learning for hammering echo

discriminant analysis in algorithm 3.1. Then, we explicit introduce the algorithms employed for this application.

**Algorithm 3.1:** ONLINELEARNING( $\mathbf{x}_t, y_t, \mathbf{w}_t$ )

**Initialization**  $\mathbf{w}_1 \leftarrow 0$

**for**  $t = 1, 2, \dots, T$

**do**  $\left\{ \begin{array}{l} \text{input hammering echo instance is received with label: } \mathbf{x}_t \in \mathcal{X}, y_t \in \mathcal{Y} \\ \text{predict label of input echo: } \hat{y}_t = \text{sign}(f(\mathbf{x}_t; \mathbf{w}_t)) \\ \text{compute the prediction loss: } l(\mathbf{w}_t; (\mathbf{x}_t; \mathbf{w}_t)) \\ \text{if } l(\mathbf{w}_t; (\mathbf{x}_t; \mathbf{w}_t)) > 0 \\ \quad \text{then update the classification model:} \\ \quad \mathbf{w}_{t+1} \leftarrow \Delta((\mathbf{w}_t; (\mathbf{x}_t; \mathbf{w}_t))) \end{array} \right.$

**return** ( $\mathbf{w}_{t+1}$ )

### 3.2.1. Perceptron

The perceptron algorithm is the initial method for online learning [20]. Given the linearly separable data, the method can convergence to a hyperplane to shatter the different classes in a finite number of updates. The prediction function of perceptron is very simple:  $\hat{y}_t = \text{sign}(\mathbf{w}^T \mathbf{x}_t)$  and the updating rule will be conducted as follows:

$$\mathbf{w}_{t+1} = \mathbf{w} + y_t \mathbf{x}_t \quad \text{if } \hat{y}_t \neq y_t \quad (3)$$

There is neither parameter nor optimization constrains in the perceptron algorithm. Perceptron algorithm has several limitations. First, it can only classify linearly separable sets of vectors. If the class-conditional data distribution is inherently nonlinear, perceptron will never reach a point where all vectors are classified properly. Second, since there is no constraint applied during model training, perceptron is vulnerable to noise. To alleviate the problems, substantial modification had been carried out. Representative works can be referred in [18].

### 3.2.2. Online Gradient Descent (OGD)

Gradient descend updating is another efficient approach for online learning [21]. In this evaluation, we selected logistic loss to measure the prediction error:

$$l(\mathbf{w}; (\mathbf{w}_t, y_t)) = \log(1 + \exp(-y_t(\mathbf{w}_t \cdot \mathbf{x}_t))) \quad (4)$$

Subsequently, the updating rule can be represented as:

$$\mathbf{w}_{t+1} = \mathbf{w}_t + \eta_t y_t \mathbf{x}_t \cdot \frac{1}{1 + \exp(y_t(\mathbf{w}_t \cdot \mathbf{x}_t))}, \quad \eta_t = C/\sqrt{t} \quad (5)$$

### 3.2.3. Passive-Aggressive Learning Algorithm[PA]

is one state-of-the-art first order online learning approach. The optimization formulation can be expressed as follows:

$$\mathbf{w}_{t+1} = \underset{\mathbf{w} \in \mathbb{R}^d}{\text{argmin}} \frac{1}{2} \|\mathbf{w} - \mathbf{w}_t\|^2, \quad \text{s.t. } l(\mathbf{w}; (\mathbf{w}_t, y_t)) \quad (6)$$

where the loss function is based on the hinge loss:

$$l(\mathbf{w}; (\mathbf{w}_t, y_t)) = \begin{cases} 0 & \text{if } y_t(\mathbf{w} \cdot \mathbf{x}_t) \geq 1 \\ 1 - y_t(\mathbf{w}_t \cdot \mathbf{x}_t) & \text{otherwise} \end{cases} \quad (7)$$

The updating rule can be derived analytically:

$$\mathbf{w}_{t+1} = \mathbf{w}_t + \eta_t^{PA} y_t \mathbf{x}_t, \quad \text{where } \eta_t^{PA} = \frac{l(\mathbf{w}_t; (\mathbf{w}_t, y_t))}{\|\mathbf{w}_t\|^2}. \quad (8)$$

164 In addition, several variants of PA method had been investigated [22]. The core idea is to add slack  
165 variable  $\xi$ -induced penalty to handle non-separable cases.

### 166 3.2.4. The Second Order Perception (SOP)

Aiming at better characterizing the hammering echo data structure, advanced second-order online learning approaches had been developed. Unlike the above-mentioned first-order algorithms, the second-order online learning is designated to exploit the underlying relationship between features. Concretely, it assumes the weight vector exhibits Gaussian distribution  $\mathbf{w} \sim \mathcal{N}(\mu, \Sigma)$ . At initialization stage, two additional hyperparameters are commonly set to  $\mathbf{w}_1 = 0, \Sigma_1 = a\mathbf{I}$ . Furthermore, the prediction function is noted as:

$$\hat{y}_t = \text{sign}(\mathbf{w}^\top \mathbf{x}_t), \quad \mathbf{w}_t = (\Sigma_t + \mathbf{x}_t \mathbf{x}_t^\top)^{-1} \mu_t \quad (9)$$

The following updating process is conducted as the predicted label is inconsistent to true label:

$$\mu_{t+1} = \mu_t + y_t \mathbf{x}_t, \quad \Sigma_{t+1} = \Sigma_t + \mathbf{x}_t \mathbf{x}_t^\top \quad (10)$$

167 A representative work for second order perception can be referred to [23].

### 168 3.2.5. The Confidence-Weighted learning algorithm (CW)

CW method is an advanced second-order online learning [24]. In contrast to SOP approach, CW methods perform the Kullback-Leibler divergence minimization between the new weight distribution and the old one with constraint that the probability of correct classification can be improved. The updating rule of CW is shown as below:

$$(\mu_{t+1}, \Sigma_{t+1}) = \underset{\mu, \Sigma}{\text{argmin}} D_{KL}(\mathcal{N}(\mu, \Sigma), \mathcal{N}(\mu_t, \Sigma_t)), \quad \text{s.t. } Pr_{\mathbf{w} \sim \mathcal{N}(\mu, \Sigma)}[y_t(\mathbf{w} \cdot \mathbf{x}_t)] \geq \eta \quad (11)$$

169 A closed-form solution can be derived as:  $\mu_{t+1} = \mu_t + \alpha_t y_t \Sigma_t \mathbf{x}_t$ ;  $\Sigma_{t+1} = \Sigma_t - \beta_t \Sigma_t \mathbf{x}_t \mathbf{x}_t^\top \Sigma_t$ , where the  
170 updating coefficients can be calculated as follows:  $\alpha_t = \max\{0, \frac{1}{v_t \zeta} (-m_t \psi + \sqrt{m_t^2 \frac{\phi^4}{4} + v_t \phi^2 \zeta})\}$ ;  $\beta_t =$   
171  $\alpha_t \phi / (\sqrt{u_t} + v_t \alpha_t \phi)$ . More detail parameters setting discussion can be found in [24].

### 172 3.2.6. Adaptive Regularization of Weight Vectors (AROW)

Regularization is regarded as useful trick to enhance both accuracy and robustness of online learning algorithm. AROW method added adaptive regularizer to restrict the sudden changes of weight during online learning[25]. The formulation of AROW is presented as follows:

$$(\mu_{t+1}, \Sigma_{t+1}) = \underset{\mu, \Sigma}{\text{argmin}} D_{KL}(\mathcal{N}(\mu, \Sigma), \mathcal{N}(\mu_t, \Sigma_t)) + \frac{1}{2\gamma} l^2(\mu; (\mathbf{x}_t, y_t)) + \frac{1}{2\gamma} \mathbf{x}_t^\top \Sigma \mathbf{x}_t \quad (12)$$

where

$$l^2(\mu; (\mathbf{x}_t, y_t)) = (\max\{0, 1 - y_t(\mu \cdot \mathbf{x}_t)\})^2 \quad (13)$$

The updating coefficients can be obtained by solving optimization problem:

$$\mu_{t+1} = \mu_t + \alpha_t \Sigma_t y_t \mathbf{x}_t, \quad \Sigma_{t+1} = \Sigma_t - \beta_t \Sigma_t \mathbf{x}_t \mathbf{x}_t^\top \Sigma_t \quad (14)$$

$$\alpha_t = l(\mu_t; (\mathbf{x}_t, y_t))\beta_t, \beta_t = \frac{1}{\mathbf{x}_t^T \Sigma_t \mathbf{x}_t + r} \quad (15)$$

### 3.2.7. Soft Confidence-Weighted Learning (SCW-II)

SCW is more advanced second-order learning algorithm that improves over the original CW by adding the capability to handle the non-separable cases, and also improves over AROW by adding the adaptive margin property [26]. The classification suffer loss for input echo data is defined as  $l_t = \max\{0, 1 - y_t \mathbf{w}_t^T \mathbf{x}_t\}$ . If  $l_t > 0$ , the classification model will be updated:

$$\mu_{t+1} = \mu_t + \alpha_t y_t \Sigma_t \mathbf{x}_t; \Sigma_{t+1} = \Sigma_t - \beta_t \Sigma_t \mathbf{x}_t \mathbf{x}_t^T \Sigma_t, \quad (16)$$

where

$$\begin{aligned} \alpha_t &= \min\{C, \max\{0, \frac{1}{v_t \zeta} (-m_t \psi + \sqrt{m_t^2 \frac{\phi^4}{4} + v_t \phi^2 \zeta})\}\}; \beta_t = \alpha_t \phi / (\sqrt{u_t} + v_t \alpha_t \phi) \\ u_t &= \frac{1}{4} (-v_t \alpha_t \phi + \sqrt{\alpha_t^2 v_t^2 \phi^2 + 4v_t})^2, v_t = \mathbf{x}_t^T \Sigma_t \mathbf{x}_t, m_t = y_t (\mu_t \cdot \mathbf{x}_t) \\ \gamma_t &= \phi \sqrt{\phi^2 m_t^2 v_t^2 + 4n_t v_t (n_t + v_t \phi^2)} \text{ and } n_t = v_t + \frac{1}{2C} \end{aligned} \quad (17)$$

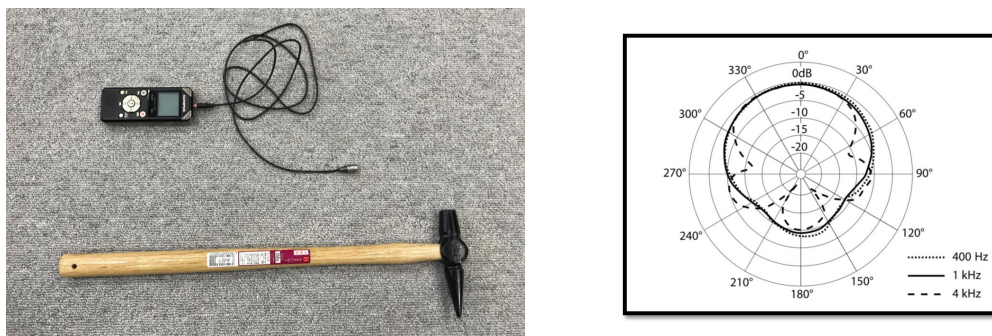
### 3.3. Hammering echo data visualization

Data visualization is widely recognized as one integral part of nowadays data analysis systems, which makes complex data more accessible, understandable and usable. In our hammering echo pattern investigation system, we incorporate data visualization function so as to let end-users browse and understand the massive echo data distributions. We adopted the fundamental method principal component analysis (PCA), which is a standard way for visualizing data. The basic principle of PCA is to find the low dimension linear subspace such that the variations of data can be maximized. The detail procedures can be found in [19]. We present the whole hammering echo data visualization results in the experimental analysis section.

## 4. Experimental Validations

### 4.1. Data Collection

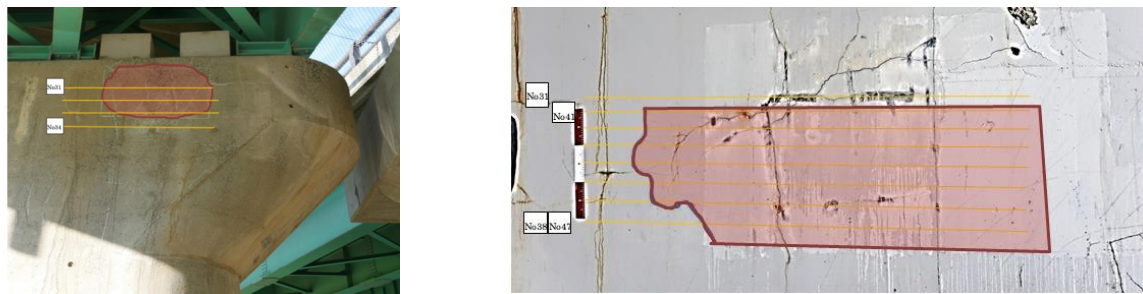
In this section, we introduce the hammering echo dataset we created to evaluate the proposed system. First, we present the impact-echo hardware we used for data collection in Figure 5. Followingly, table 1 shows more detail specifications. For echo data recording, the sampling rate was set to 44.1kHz and resolution was fixed to 16-bit depth.



**Figure 5.** The low-cost impact-echo system (left) and microphone directivity illustration (right)

**Table 1.** Summary of the parameter setting by algorithms

	Device	Specification
1	Hammer	Inspection handy hammer: 420mm long and 200 gram weight
2	Transducer	Low-cost condenser microphone: ECM PC60
3	Recorder	Olympus Voice-Trek V-803

**Figure 6.** Photos of two working sites for hammering echo data capture

We visited 12 inspection sites to capture echo data. Meanwhile, binary expert annotations, i.e. one echo indicating normal or anomalous conditions, has also been collected. In figure 6, we show the photos of two inspection sites. The defective area had been tagged with pink color by inspector. In addition, we marked multiple parallel lines in yellow, which explains the trace of hammering. Scanning speed was around 80 centimeter per minute (cm/min). The hammering area varies with locations. As a result, we obtained 10940 annotated echo instances, among which 9349 are normal and 1591 are anomalous instances, respectively. The dataset laid fundamentals for further numerical analysis.

#### 4.2. Experimental settings

At echo feature extraction stage, we determine the Fourier analysis window length to be 1024. Band pass filter is applied to focus on the frequencies ranging from 500 to 15000Hz. At online learning stage, parameter tuning plays a key role in achieving accurate hammering echo pattern classification. In this study, we evaluate 7 state-of-the-art online learning approaches with the massive real hammering echo data. The detail parameter settings are presented in Tab. 1.

**Table 2.** Summary of the parameter setting by algorithms

Index	Algorithm	C	$\alpha$	$\eta$	Others
1	Perceptron	/	/	/	parameter free
2	OGD	$C = 1$	/	/	$\eta_t = C/\sqrt{t}$
3	PA	/	/	/	parameter free
4	SOP	/	$\alpha = 1$	/	parameter free
5	CW	/	$\alpha = 1$	$\eta = 0.7$	$\Sigma = a * I$
6	AROW	$C = 1$	$\alpha = 1$	/	$r = C, \Sigma = \alpha * I$
7	SCW-II	$C = 1$	$\alpha = 1$	$\eta = 0.75$	$\Sigma = a * I$

The first parameter  $C$  governs the trade-off between the fitting loss term and regularization term in machine learning model training. In the second order algorithms, the parameter  $\alpha = 1$  is used to initialize the covariance matrix, i.e.  $\Sigma = \alpha * I$ , where  $I$  is identity matrix. Parameter  $\eta$  is used to define loss function in the confidence-weighted learning algorithms, i.e. in CW and SCW-II. The

experiments had been performed in the same vein as real scenario, in which the labeled data was fed to online learning system in a sequential manner. The experiments were conducted over 20 random permutations for the whole echo dataset. At each iteration, we divided the dataset into 15 sub data sets. During online learning, we recorded the evaluation results, i.e. echo classification accuracies and computation time costs, when one subset had been processed. Those information will help us understand the learning behavior of algorithm. Finally, the results are presented by averaging of total 20 trials.

#### 4.3. Echo Data Visualization

As introduced in section 3.3, data visualization is useful approach to understand the data. In figure. 6, we present the distribution of echo dataset using principal component analysis (PCA). In the visualization, binary class labels were noted with different colors, i.e. the normal echoes were marked with black and flaw-induced ones were colored in red. According to the distribution plot, we have several major findings: 1. damage-induced echoes produced more scattered distribution compared to that of healthy ones. It is reasonable because the damaged concrete usually generated more complex echo spectrum. 2. The boundary between normal and anomalous echoes is not clear; in other words, there exists strong non-linearity between the two-class distribution. From the machine learning aspect, the methods which were designated to deal with the inherently nonlinear data may perform superiorly. Grounded on above understanding to the data collection, we start the algorithmic analysis as follows.

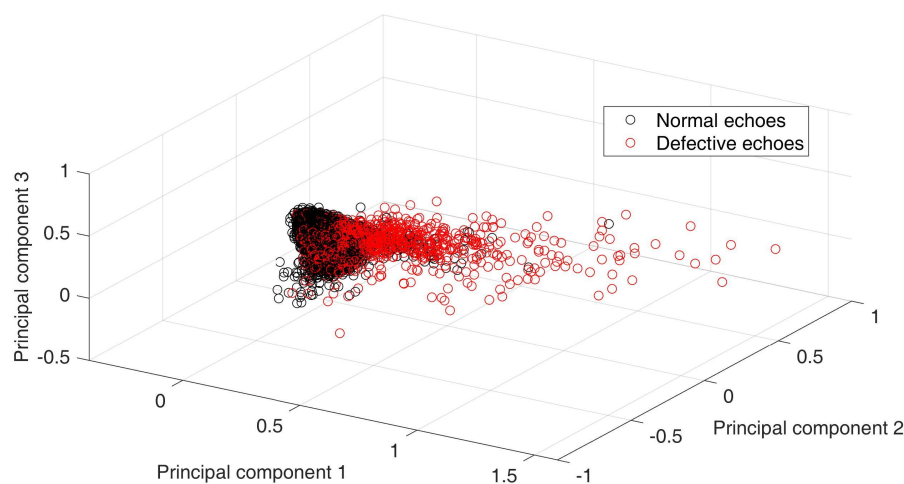


**Figure 7.** Visualization of hammering echo dataset using principal component analysis (PCA)

#### 4.4. Empirical Evaluation Results

In this part, we present results of experimental validation. The comparison has been drawn of three aspects: echo pattern classification accuracy, processing efficiency and computation complexity. As for the first comparison—accuracy, we adopted two metrics: mistake rate transition curve and the cumulative classification error rate. It can be anticipated that with more data being examined, the mistake rate would decrease monotonically. To exploit the performance of online echo analysis models, we presented the cumulative error rate after the whole online learning process was done. Figure 7 exhibited the overall errors statistics during online learning process. First of all, by examining the overall mistakes, we found that second-order algorithms, i.e. SOP, CW, AROW and SCW-II usually outperforms first-order algorithms, including perception, OGD and PA; also margin based algorithms, such as CW and SCW-II, usually outperforms non-margin based methods.

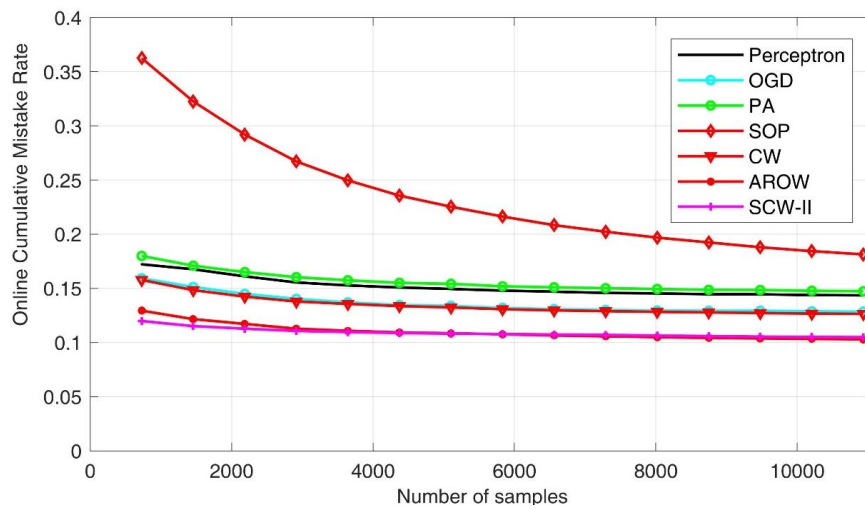


**Figure 8.** Summary of online cumulative classification error rate

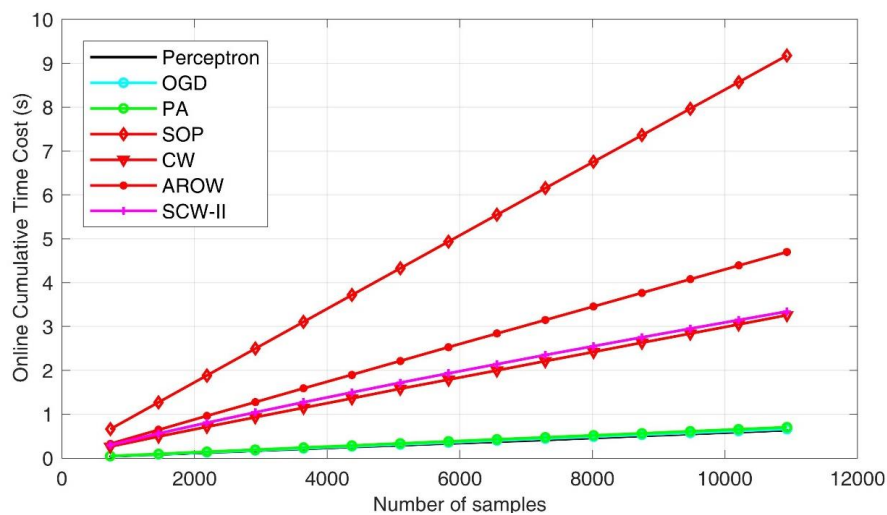


**Figure 9.** Processing time cost comparison

As for the second evaluation criteria—computation efficiency, we presented the cumulative time costs for all the seven online learning algorithms under evaluation in figure 8. We found that the first-order schemes exhibited superior efficiency due to simpler formulation. The SOP method took longest time in process, which is one of initial second order approaches. confident-weighted learning methods, including both CW and SCW, achieved favorable performance in balancing accuracy and efficiency. To demonstrate the complexity of online learning algorithms, we further showed cumulative number of updates. In general, fewer update steps indicates the algorithm is efficient to establish more robust pattern classification hyperplane such that input feature distribution shift can be accommodated. By examining figure 9, we can see first order methods usually produced smaller number of updates. However, the classification accuracies were inferior. AROW scheme made significantly larger number of updates, which can induce high time cost in processing.

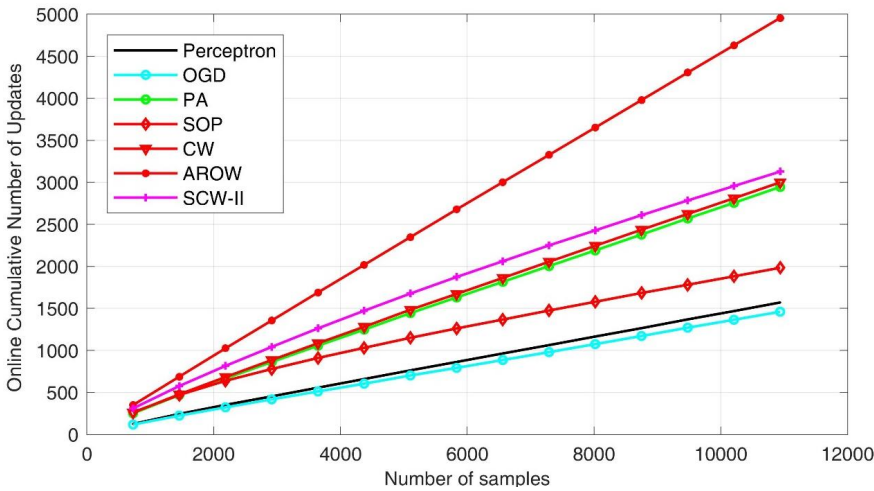


**Figure 10.** Comparison of number of updating steps

247 To clarify the comparison, we further prepared table 2 to summarize the key experimental results,  
248 including cumulative mistake rate, size of support vectors (SVs) and cpu run time. Such quantitative  
249 information is complementary to above charts. From the table, we found that SCW-II outperformed  
250 all other methods in echo pattern classification accuracy. Meanwhile, the method achieved superior  
251 efficiency among all the second order online learning algorithms. Besides, we also investigated the  
252 number of support vectors (SVs) used by different learning scheme. SVs are defined as the samples  
253 used to determined max-margin hyperplane for classification. Since the echo data is highly non-linear,  
254 we can see larger number of SVs had been used at classification stage.

**Table 3.** Summary of all experimental results

Algorithm:	(mistake rate (m+/-std))	size of SVs (m+/-std)	cpu time (m+/-std))
Perceptron	0.144 ± 0.002	1570.8 ± 25.2	0.647 ± 0.056
OGD	0.128 ± 0.005	1460.7 ± 59.3	0.718 ± 0.045
PA	0.147 ± 0.002	2945.8 ± 41.2	0.699 ± 0.037
SOP	0.181 ± 0.002	1983.8 ± 27.0	9.708 ± 0.608
CW	0.126 ± 0.002	3000.1 ± 36.6	3.460 ± 0.248
AROW	0.115 ± 0.004	6378.9 ± 278.2	6.357 ± 0.429
SCW-II	0.105 ± 0.002	3128.4 ± 61.6	3.577 ± 0.244

255 As a result, among all the compared algorithms, SCW-II produced the best performance in terms  
256 of accuracy; for other metrics including number of updates, and running time cost, it also outperformed  
257 other second order methods. Therefore, the method can be optimal selection for the application of  
258 hammering echo online learning. It is noteworthy that errors may exist in the echo labels, because  
259 practical hammering inspection usually takes location information into account. It can be regarded as  
260 performing region-based smoothing over each individual expert echo labels nearby. In contrast, our  
261 quantitative evaluation had been conducted in a point-wise way. Such factor can be one major reason  
262 that lead to the error rate over 10%. The empirical evaluation validated the effectiveness of online  
263 learning approach for hammering echo pattern investigation.

264 **5. Conclusions**

265 In this paper, we attempted to develop an efficient learning framework which can mimic human  
266 performance on hammering echo data investigation. Field inspectors determined health condition of  
267 concrete by using auditory perception of hammering echoes. In this study, we formulate such process

using binary classification. Moreover, in order to deal with large-scale hammering echo data, we employed online learning algorithm which can update itself so as to minimize the cumulative error rate as echo data and label are received. To validate the proposed system, we created a hammering echo dataset with professional annotations and the experimental result demonstrated the effectiveness of proposed echo data learning system. In next stage of this research, we hope to update the hardware part, such as employing wireless/wearable MIC, and collect more data to further enhance the data analysis accuracy for real applications.

## 6. Author Contributions

Jiaxing YE provided the method and conducted the experiments. Takumi Kobayashi was in charge of experiment design and parameter optimization. Masaya Iwata helped in the collection and organization of data. Hiroshi Tsuda and Masahiro Murakawa supervised the theoretical statement of the problem. All authors revised the paper for intellectual content.

## 7. Acknowledgement

This study was partly supported by Cross-ministerial Strategic Innovation Promotion Program (SIP) / Technologies for maintenance, renewal, and management for infrastructure, and supported by the New Energy and Industrial Technology Development Organization (NEDO), Japan. The authors would like to thank the anonymous reviewers for their valuable comments and suggestions to improve the quality of the paper.

## 8. Conflicts of Interest

The authors declare no conflict of interest..

## References

1. Sansalone, Mary J., William B. Streett. Impact-echo. *Nondestructive evaluation of concrete and masonry*, Publishing House: Bullbrier Press, Jersey Shore, PA USA, **1997**
2. Schubert F, Kohler B. Ten lectures on impact-echo. *Journal of Nondestructive Evaluation*, **2008**, 27, pp. 5-21.
3. Carino N J, Sansalone M, Hsu N N. A point source-point receiver, pulse-echo technique for flaw detection in concrete. *Journal of Amercian Concrete Institute*, **1986**, 2, pp. 199-208.
4. Farrar, Charles R., Keith Worden. Structural health monitoring: a machine learning perspective. John Wiley Sons, **2012**.
5. PoLiang Yeh, PeiLing Liu, Application of the wavelet transform and the enhanced Fourier spectrum in the impact echo test, *In NDT International*, **2008** , 41, pp. 382-394, ISSN 0963-8695.
6. Sansalone M. Impact-echo: The complete story. *Structural Journal*, **1997**, 94, pp. 777-786.
7. Jinying Zhu, Popovics S. John, Imaging concrete structures using air-coupled impact-echo, *Journal of engineering mechanics*, **2007**, 133.6, pp. 628-640.
8. R. Groschup, C.U. Grosse, Development of an Efficient Air-Coupled Impact-Echo Scanner for Concrete Pavements. *In Proceedings of World Conference on Non-Destructive Testing*, **2016**.
9. Gibson, Alexander, John S. Popovics, Lamb wave basis for impact-echo method analysis. *Journal of Engineering mechanics* **2005**, 131.4, pp. 438-443.
10. Hola, Jerzy, Lukasz Sadowski, and Krzysztof Schabowicz. Nondestructive identification of delaminations in concrete floor toppings with acoustic methods. *Automation in Construction*, **2011**, 20.7, pp.799-807.
11. Jorge Igual, Addisson Salazar, Gonzalo Safont, Luis Vergara. Semi-supervised Bayesian classification of materials with impact-echo signals. *Sensors*, **2015**, 15.5, pp.11528-11550.
12. Sadowski, Lukasz. Non-destructive identification of pull-off adhesion between concrete layers. *Automation in Construction*, **2015**, 57, pp.146-155.
13. Li Bing, K. Ushiroda, L. Yang, Q. Song, J. Xiao. Wall-climbing robot for non-destructive evaluation using impact-echo and metric learning SVM, *International Journal of Intelligent Robotics and Applications* **2017**, 1.3, pp. 255-270.

- 314 14. Zhang, Jing-Kui, Weizhong Yan, De-Mi Cui. Concrete condition assessment using impact-echo method and  
315 extreme learning machines. *Sensors*, **2016**, 16.4, 447
- 316 15. Jiaying Ye, Kobayashi Takumi, Masaya Iwata, Masahiro Murakawa, Tetsuya Higuchi, T. Kubota, T. Yui.  
317 Noise Reduction Methods for Hammering Impact Acoustic Inspection: An Experimental Comparison. In  
318 Proceedings of the International Conference on Structural Health Monitoring, **2015**.
- 319 16. Jiaying Ye, Kobayashi Takumi, Masaya Iwata, Masahiro Murakawa. Noise robust hammering echo analysis  
320 for concrete structure assessment under mismatch conditions: A sparse coding approach. In *Proceedings of*  
321 *the IEEE Sensors Applications Symposium (SAS)*, **2017**, pp. 1-6
- 322 17. Alexander Gepperth, Barbara Hammer, Incremental learning algorithms and applications, In *Proceedings of*  
323 *European Symposium on Artificial Neural Networks (ESANN)*, **2016**, pp. 357-368.
- 324 18. Hoi Steven CH, Jialei Wang, and Peilin Zhao, Libol: A library for online learning algorithms, *The Journal of*  
325 *Machine Learning Research*, **2014**, 15.1, pp. 495-499.
- 326 19. Christopher M Bishop, Pattern Recognition and Machine Learning, Springer Science Business Media, **2006**
- 327 20. Frank Rosenblatt. The perceptron: A probabilistic model for information storage and organization in the  
328 brain. *Psych. Review*, **1958**, 7, 551–585.
- 329 21. M. Zinkevich. Online convex programming and generalized infinitesimal gradient ascent. In *Proceedings of*  
330 *the International conference on machine learning (ICML)*, **2003**, pp. 928–936.
- 331 22. K. Crammer, O. Dekel, J. Keshet, S. Shalev-Shwartz, and Y. Singer. Online passive aggressive algorithms.  
332 *Journal of Machine Learning Research*, **2006**, 7, 551–585.
- 333 23. Cesa-Bianchi, Nicolo, Alex Conconi, Claudio Gentile. A second-order perceptron algorithm. *SIAM Journal*  
334 *on Computing*, **2005**, 34.3, pp.640-668.
- 335 24. K. Crammer, M. Dredze, and F. Pereira. Exact convex confidence-weighted learning. In *Proceedings of the*  
336 *Neural Information Processing System Conference (NIPS)*, **2008**, pages 345–352.
- 337 25. K. Crammer, A. Kulesza, and M. Dredze. Adaptive regularization of weight vectors. In *Proceedings of the*  
338 *Neural Information Processing System Conference (NIPS)*, **2009**, pages 414–422.
- 339 26. Jialei Wang, Peilin Zhao, and Steven C. H. Hoi. Confidence-weighted linear classification. In *Proceedings of*  
340 *the International conference on machine learning (ICML)*, **2012**, pp. 121-128.